Effect of the Lorentz force on on-off dynamo intermittency

Alexandros Alexakis and Yannick Ponty
Université de Nice Sophia-Antipolis, France (UNS),
Centre National de la Recherche Scientifique (CNRS),
and Observatoire de la Côte d'Azur, Boîte Postale 4229, Nice Cedex 04, France
(Received 28 September 2007; published 14 May 2008)

An investigation of the dynamo instability close to the threshold produced by an *ABC* forced flow is presented. We focus on the on-off intermittency behavior of the dynamo and the countereffect of the Lorentz force in the nonlinear stage of the dynamo. The Lorentz force drastically alters the statistics of the turbulent fluctuations of the flow and reduces their amplitude. As a result, much longer bursts (on phases) are observed than is expected based on the amplitude of the fluctuations in the kinematic regime of the dynamo. For large Reynolds numbers, the duration time of the on phase follows a power law distribution, while for smaller Reynolds numbers the Lorentz force completely kills the noise and the system transits from a chaotic state into a laminar time periodic flow. The behavior of the on-off intermittency as the Reynolds number is increased is also examined. The connections with dynamo experiments and theoretical modeling are discussed.

DOI: 10.1103/PhysRevE.77.056308 PACS number(s): 47.65.−d, 47.20.Ky, 47.27.Sd, 52.65.Kj

I. INTRODUCTION

Dynamo action, the self-amplification of a magnetic field due to the stretching of magnetic field lines by a flow, is considered to be the main mechanism for the generation of magnetic fields in the universe [1]. In that respect many experimental groups have successfully attempted to reproduce dynamos in liquid sodium laboratory experiments [2–8]. The induction experiments [9–18] studying the response of an applied magnetic field inside a turbulent metal liquid also represent challenging science. With or without dynamo instability, the flow of a conducting fluid forms a complex system, with a large number of degrees of freedom and a wide range of nonlinear behaviors.

In this work we focus on one special behavior: the on-off intermittency or blowout bifurcation [19,20]. On-off intermittency is present in chaotic dynamical systems for which there is an unstable invariant manifold in the phase space such that the unstable solutions have a growth rate that varies strongly in time, taking both positive and negative values. If the averaged growth rate is sufficiently smaller than the fluctuations of the instantaneous growth rate, then the solution can exhibit on-off intermittency where bursts of the amplitude of the distance from the invariant manifold are observed (when the growth rate is positive) followed by a decrease of the amplitude (when the growth rate is negative). (See [21,22] for a more precise definition.)

On-off intermittency has been observed in different physical experiments including electronic devices, electrohydrodynamic convection in nematics, gas discharge plasmas, and spin-wave instabilities [23]. In the magnetohydrodynamics (MHD) context, near the dynamo instability onset, the on-off intermittency has been investigated by modeling of the Bullard dynamo [24]. Using direct numerical simulation [21,22], they were able to observe on-off intermittency solving the full MHD equations for the ABC dynamo (here we present an extended study of this particular case). on-off intermittency has also been found recently for a Taylor-Green flow [25]. Finally, recent liquid metal experimental results [26] show some intermittent behavior, with features reminiscent of on-off self-generation that motivated our study.

For the MHD system we are investigating the evolution of the magnetic energy $E_b=\frac{1}{2}\int \mathbf{b}^2 dx^3$ which is given by $\partial_t E_b=\int \mathbf{b}(\mathbf{b}\cdot\boldsymbol{\nabla})\mathbf{u}-\eta(\boldsymbol{\nabla}\times\mathbf{b})^2 dx^3$, where $\mathbf{b}$ is the magnetic field and $\mathbf{u}$ is the velocity field. If the velocity field has a chaotic behavior in time the right-hand side of the equation above can take positive or negative values and can be modeled as multiplicative noise. A simple way is to model the behavior of the magnetic field during the on-off intermittency using a stochastic differential equation (SDE) [19,20,27–35]:

$$\partial_t E_b = (a+\xi)E_b - Y_{\mathrm{NL}}(E_b), \tag{1}$$

where E_b is the magnetic energy, a is the long-time-averaged growth rate, and ξ models the noise term typically assumed to be white (see, however, [34,35]) and of amplitude D such that $\langle \xi(t)\xi(t')\rangle = 2D\delta(t-t')$. Y_{NL} is a nonlinear term that guarantees the saturation of the magnetic energy to finite values typically taken to be $Y_{\mathrm{NL}}(X)=X^3$ for investigations of supercritical bifurcations or $Y_{\mathrm{NL}}(X)=X^5-X^3$ for investigations of subcritical bifurcations. Alternative, an upper no-flux boundary is imposed at $E_b=1$. In all these cases (independent of the nonlinear saturation mechanism) the above SDE leads to a stationary distribution function that for $0<a<D$ has a singular behavior at $E_b=0$: $P(E_b)\sim E_b^{a/D-1}$, indicating that the systems spends a lot of time in the neighborhood of $E_b=0$. This singularity is the signature of on-off intermittency. Among other predictions of the SDE model, here we note that the distribution of the duration time of the off phases follows a power law behavior $f_{\mathrm{PDF}}(\Delta T_{\mathrm{off}})\sim \Delta T_{\mathrm{off}}^{-1.5}$, all moments of the magnetic energy follow a linear scaling with a, $\langle E_b^m\rangle \sim a$, and for $a=0$ the set of bursts has a fractal dimension $d=1/2$ [30–33].

In this dynamical system Eq. (1), however, the noise amplitude and the noise properties do not depend on the amplitude of the magnetic energy. However, in the MHD system, when the nonlinear regime is reached, the Lorentz force has

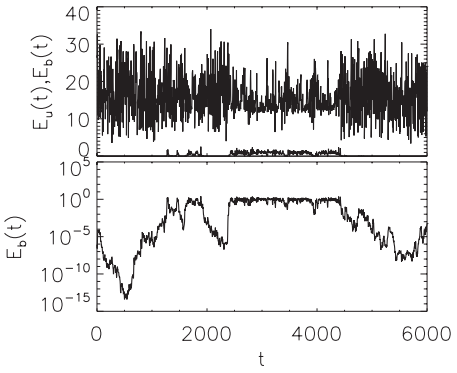

FIG. 1. A typical example of a burst. The top panel shows the evolution of the kinetic energy (top line) and magnetic energy (bottom line). The bottom panel shows the evolution of the magnetic energy in a log-linear plot. During the on phase of the dynamo the amplitude of the noise of the kinetic energy fluctuations is significantly reduced. The runs were for the parameters Gr=39.06 and G_M=50.40.

clear effects on the flow, such as the decrease of the small-scale fluctuation, and the decrease of the local Lyapunov exponent [36,37]. In some cases, the flow is altered so strongly that the MHD dynamo system jumps into another attractor, which can no longer sustain the dynamo instability [38]. Although the exact mechanism of the saturation of the MHD dynamo is still an open question that might not have a universal answer, it is clear that both the large scales and the turbulent fluctuations are altered in the nonlinear regime and need to be taken into account in a model.

Figure 1 demonstrates this point, by showing the evolution of the kinetic and magnetic energy as the dynamo goes through on and off phases. During the on phases, although the magnetic field energy is an order of magnitude smaller than the kinetic energy, both the mean value and the amplitude of the observed fluctuations of the kinetic energy are significantly reduced. As a result the on phases last a lot longer than the SDE model would predict. With our numerical simulations, we aim to describe which of the on-off intermittency properties are affected through the Lorentz force feedback.

This paper is structured as follows. In Sec. II we discuss the numerical method used. In Sec. III A we present a table of our numerical runs and discuss the dynamo onset. Results for small Reynolds numbers showing the transition from a laminar dynamo to on-off intermittency are presented in Sec. III B, and the results on fully developed on-off intermittency behavior are given in Sec. III C. Conclusions, and implications for modeling and for laboratory experiments are given in the last section.

II. NUMERICAL METHOD

Our investigation is based on the numerical integration of the classical incompressible magnetohydrodynamic equations (2) in a full three-dimensional periodic box of size 2π, with a parallel pseudospectral code. The MHD equations are

$$\partial_t \mathbf{u} + \mathbf{u}\cdot\nabla\mathbf{u} = -\nabla P + (\nabla\times\mathbf{b})\times\mathbf{b} + \nu\nabla^2\mathbf{u} + \mathbf{f},$$

$$\partial_t \mathbf{b} = \nabla\times(\mathbf{u}\times\mathbf{b}) + \eta\nabla^2\mathbf{b}, \tag{2}$$

along with the divergence-free constraints $\nabla\cdot\mathbf{u}=\nabla\cdot\mathbf{b}=0$, where $\mathbf{u}$ is the velocity, $\mathbf{b}$ is the magnetic field (in units of the Alfvén velocity), ν is the molecular viscosity, and η is the magnetic diffusivity. $\mathbf{f}$ is an externally applied force that in the current investigation is chosen to be the *ABC* forcing [39] explicitly given by

$$\mathbf{f} = \{\hat{x}[A\sin(k_z z) + C\cos(k_y y)], \quad \hat{y}[B\sin(k_x x) + A\cos(k_z z)], \quad \hat{z}[C\sin(k_y y) + B\cos(k_x x)]\}, \tag{3}$$

with all the free parameters chosen to be 1: $A=B=C=k_x=k_y=k_z=1$.

The MHD equations have two independent control parameters that are generally chosen to be the kinetic and magnetic Reynolds numbers defined by: $\mathrm{Re}=UL/\nu$ and $R_M=UL/\eta$, respectively, where U is chosen to be the root mean square of the velocity (defined by $U=\sqrt{2E_u/3}$, where E_u is the total kinetic energy of the velocity) and L is the typical large scale here taken as $L=1.0$. Alternatively, we can use the amplitude of the forcing to parametrize our system, in which case we obtain the kinetic and magnetic Grashof numbers $\mathrm{Gr}=FL^3/\nu^2$ and $G_M=FL^3/\nu\eta$, respectively. Here F is the amplitude of the force, which is taken to be unity $F=\sqrt{(A^2+B^2+C^2)/3}=1$ following the notation of [53].

We note that in the laminar limit the two different sets of control parameters are identical, Gr=Re and $G_M=R_M$, but in the turbulent regime (where the forcing is balanced by the nonlinear term $F\sim U^2/L$) the scaling $\mathrm{Gr}\sim\mathrm{Re}^2$ and $G_M\sim\mathrm{Re}R_M$ is expected. In the examined parameter range the velocity field fluctuates in time, generating uncertainties in the estimation of the root mean square of the velocity, and thus the Reynolds numbers as well. For this reason, in this work we are going to use the Grashof numbers as the control parameters of our system. Even though this forcing parameter is not necessarily linear with the Reynolds number, to simplify the discussion, we will used in the following text the term "Reynolds numbers" instead of "Grashof numbers," keeping the Grashof number symbols.

Starting with a statistically saturated velocity, we investigate the behavior of the kinetic and magnetic energy in time by introducing a small magnetic seed at $t=0$ and letting the system evolve. When the magnetic Reynolds (Reynolds) number is sufficiently large, the magnetic energy grows exponentially in time, reaching the dynamo instability. We have computed the dynamo onset for different kinematic Reynolds numbers (Sec. III A) starting from small Gr=11.11, for which the flow exhibits laminar *ABC* behavior, to larger values of Gr (up to Gr=625.0) that the flow is relatively turbulent.

Typical durations of the runs were 10^5 turnover times although in some cases even much longer integration time was used. For each run during the kinematic stage of the dynamo the finite-time growth rate $a_\tau(t)=\tau^{-1}\ln[E_b(t+\tau)/E_b(t)]$ was measured. The long-time-averaged growth rate was then determined as $a=\lim_{\tau\to\infty} a_\tau(0)$ and the amplitude of the noise D was measured based on $D=\tau\langle(a-a_\tau)^2\rangle/2$ (see [21,22]). A typical value of τ was 100 while for long-time averages the

TABLE I. Parameters used in the simulations. G_{Mc} is the critical magnetic Reynolds number where the dynamo instability begins and G_{Mo} is the critical magnetic Reynolds number where the dynamo instability stops having on-off behavior. Thus, on-off intermittency is observed in the range $G_{Mc} < G_M < G_{Mo}$.

Run	ν	Gr	Re	G_{Mc}	G_{Mo}
I	0.30	11.11	11.11	8.89–17.8, 24.0	8.89
II	0.28	12.75	12.75/11.22	8.50	8.50
III	0.25	16.00	14.82	9.35	9.35
IV	0.22	20.66	16.92	11.3	11.8
VI	0.20	25.00	18.45	29.4	56.8
VII	0.18	30.86	19.47	37.0	50.5
VII	0.16	39.06	20.60	48.0	59.5
VII	0.08	156.25	34.08	123.7	137.
VII	0.04	625.00	67.20	327.2	362.

typical averaging time ranged from 10^4 to 10^5 depending on the run. The need for long computational time in order to obtain good statistics restricted our simulations to low resolutions that varied from 32^3 (for $\mathrm{Gr} \leq 40.0$) to 64^3 (for $\mathrm{Gr} > 40$).

III. NUMERICAL RESULTS

A. Dynamo onset

The *ABC* flow is a strongly helical Beltrami flow with chaotic Lagrangian trajectories [40]. The kinematic dynamo instability of the *ABC* flow, even with one of the amplitude coefficients set to zero ($2^{1/2}D$ flow) [41,42] has been studied intensively [43–47], especially for fast dynamo investigation [48–52]. In the laminar regime and for the examined case where all the parameters of the *ABC* flow are equal to unity [Eqs. (4)], the flow is a dynamo in the range $8.9 \lesssim G_M \lesssim 17.8$ and for $24.8 < G_M$ [43,44]. In this range the magnetic field is growing near the stagnation point of the flow, producing cigar-shaped structures aligned along the unstable manifold.

As the kinematic Reynolds number is increased, a critical value is reached ($\mathrm{Gr}=\mathrm{Re} \sim 13$) where the hydrodynamic system becomes unstable. After the first bifurcation, further increase of the kinematic Reynolds number leads the system to jump to different attractors [53–56], until finally the fully turbulent regime is reached.

The on-off intermittency dynamo has been studied with the *ABC* forcing by [21,22]. These studies were focused on a single value of the Reynolds number while the magnetic Reynolds number was varied. We expand this work by varying both parameters. For each kinematic Reynolds number, a set of numerical runs were performed varying the magnetic Reynolds number. The different Reynolds numbers examined are shown in Table I. The case examined in [21,22] is closest to the set of runs with $\mathrm{Gr}=39.06$ although here examined at higher resolution.

First, we discuss the dynamo onset. For each kinetic Reynolds number the critical magnetic Reynolds number G_{Mc} is found and recorded in Table I. For our lowest kinematic Reynolds number $\mathrm{Gr}=11.11$, which corresponds to a slightly smaller value than the critical value for the presence of hydrodynamic instabilities, the flow is laminar and the two windows of dynamo instability [43,44] are rediscovered, as shown in Fig. 2. At higher Reynolds number, the hydrodynamic system is no longer stable, and the two windows of dynamo modes disappear, collapsing to only one (see Fig. 2). There is certainly some symmetry breaking effect in this merging [56]. The critical magnetic Reynolds number is increasing with the Reynolds number Fig. 2, and saturates at very large values of Gr [57] that are far beyond the range examined in this work.

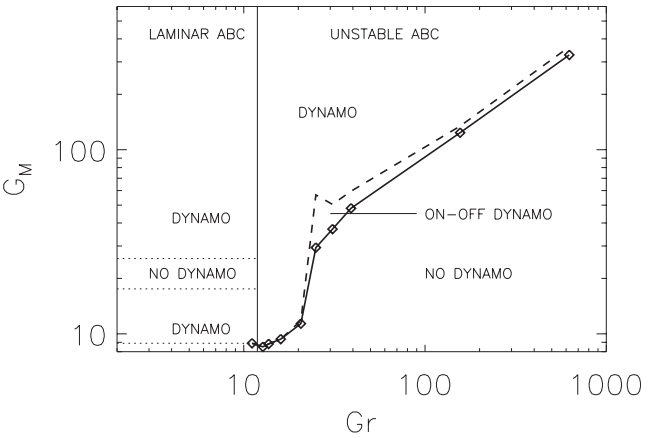

FIG. 2. Critical magnetic Reynolds number G_{Mc} above which the dynamo instability is observed (solid line) and the critical magnetic Reynolds number G_{Mo} where the on-off intermittency disappears (dashed line).

B. Route to on-off intermittency

The first examined Reynolds number beyond the laminar regime is $\mathrm{Gr}=12.75$ (run II). In this case two stable solutions of the Navier-Stokes equations coexist. Depending on the initial condition, this hydrodynamic system converges into one of the two attractors. The two velocity fields have different critical magnetic Reynolds numbers. The first solution is the laminar flow, which shares the same dynamo properties as the smaller Reynolds number flows. For the second flow, however, the previous stable window between $G_M \simeq 17.8$ and 24.0 disappears and the critical magnetic Reynolds number now becomes $G_{Mc}=8.50$, resulting in only one instability window. Figure 3 demonstrates the different dynamo properties of the two solutions. The evolution of the kinetic and magnetic energy of two runs is shown with the same parameters Gr, G_M but with different initial conditions for the velocity field. G_M is chosen in the range of the no-dynamo window of the laminar *ABC* flow.

This choice of Gr, although it exhibits interesting behavior, does not give on-off intermittency since both hydrodynamic solutions are stable in time. The next examined Reynolds number (III) gives a chaotic behavior of the hydrodynamic flow and accordingly a "noisy" exponential growth rate for the magnetic field.

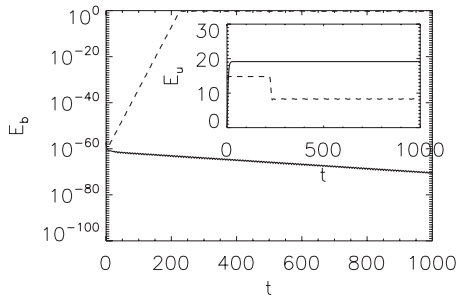

FIG. 3. Kinetic (inset) and magnetic energy for the run with Gr=12.75 and G_M=22.32 for two runs starting with different initial conditions for the velocity field. The first flow (solid line) is attracted to the laminar *ABC* flow and gives no dynamo. The second flow (dashed line) is attracted to a new solution that gives a dynamo.

The evolution of the kinetic and magnetic energy in the kinematic regime is shown in Fig. 4 for a relatively short time interval. The kinetic energy "jumps" between the values of the kinetic energy of the two states that were observed to be stable at smaller Reynolds numbers in a chaotic manner. Accordingly, the magnetic energy grows or decays depending on the state of the hydrodynamic flow, in a way that very much resembles a biased random walk in the log-linear plane. Thus, this flow is expected to be a good candidate for on-off intermittency that could be modeled by the SDE model equations given in Eq. (1). However, this flow did not result in on-off intermittency for all examined magnetic Reynolds numbers, even for the runs where the measured growth rate and amplitude of the noise were found to satisfy the criterion $a/D<1$ for the existence of on-off intermittency. What is found instead is that at the linear stage the magnetic field grows in a random way but in the nonlinear stage the solution is trapped in a stable periodic solution and remains there throughout the integration time. This behavior is demonstrated in Fig. 5, where the evolution of the magnetic energy is shown both in the linear and in the nonlinear regime.

Another interesting feature of this case is subcriticality [25]. The periodic solution that the dynamo simulations converged to in the nonlinear stage appears to be stable even for the range of G_M where no dynamo exists. Figure 6 shows the time evolution of two runs with the same parameters Gr, G_M,

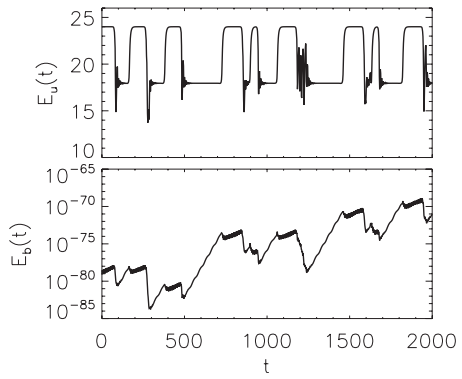

FIG. 4. Evolution of the kinetic (top panel) and magnetic (bottom panel) energy for the run with Gr=16.0 and G_M=9.39.

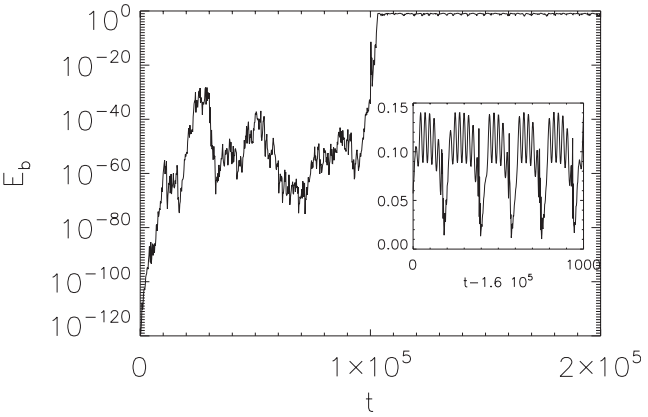

FIG. 5. Evolution of the magnetic energy for the run with Gr=16.0 and G_M=9.39. At the linear stage the logarithm of the magnetic energy grows as a random walk. At the nonlinear stage, however, the solution is trapped in a stable time-periodic solution. The inset shows the evolution of the magnetic energy in the nonlinear stage in a much shorter time interval. The examined run has $a/D=0.022<1$.

one starting with very small amplitude of the magnetic field and one starting using the output from one of the successful dynamo runs in the nonlinear stage. Although the magnetic energy of the first run decays with time, the nonlinear solution appears to be stable.

The next examined Reynolds number G=20.66 (IV) appears to be a transitory state between the previous example and the on-off intermittency that is examined in the next section. Figure 7 shows the evolution of the magnetic energy for three different values of G_M=20.66, 12.0, 11.6 for all of which the ratio a/D was measured and was found to be smaller than unity, and therefore they are expected to give on-off intermittency based on the SDE model. Only the bottom panel, however (which corresponds to the value of G_M=11.6 closest to the onset value G_M=11.3), shows on-off intermittency. A singular power law behavior of the probability distribution function (PDF) of the magnetic energy during the off phases (small E_b) for the last run was observed to be in good agreement with the predictions of the SDE. This is expected, since for small E_b the Lorentz force that is responsible for trapping the solution in the nonlinear stage does not play any role.

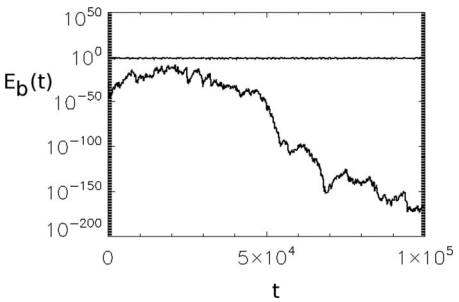

FIG. 6. Subcritical behavior of the *ABC* dynamo. The evolution of the magnetic energy for two runs with Gr=16.0 and G_M=9.30, starting with a small-amplitude magnetic field (bottom line) and starting with an amplitude of the magnetic field at the nonlinear stage (top, almost horizontal, line).

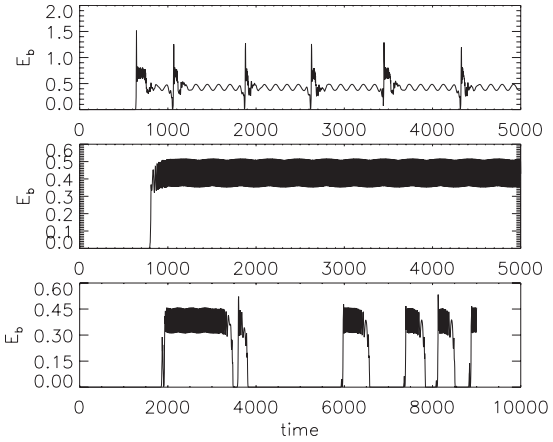

FIG. 7. Evolution of the magnetic energy for Gr=20.66 and G_M=20.66 (top panel), 12.0 (middle panel), and 11.6 (bottom panel).

C. On-off intermittency

All the larger Reynolds numbers examined display on-off intermittency and there is no trapping of the solutions in the on phase. Figure 8 shows an example of the on-off behavior for Gr=25.0 and three different values of G_M [G_M=41.6 (top panel), 35.7 (middle panel), and 31.2 (bottom panel)].

As the critical value of G_M is approached, the on phases of the dynamo (bursts) become more and more rare, as the SDE model predicts. Note, however, that the on phases of the dynamo last considerably longer. In fact, the distribution of the durations of the on phase ΔT_{on} is fitted best to a power law distribution rather than the exponential that a random walk model with an upper no-flux boundary would predict, as can be seen in Fig. 9.

The effect of the long duration of the on times can also be seen in the PDFs of the magnetic energy. The PDFs for Gr=25 for the examined G_M are shown in Fig. 10. For values of G_M much larger than the critical value G_{Mc}, the PDF of the amplitude of the magnetic field is concentrated at large values $E_b \simeq 1$, producing a peak in the PDF curves. As G_M is decreased, approaching G_{Mc} from above, a singular behavior of the PDF appears with the PDF having a power law behavior $\sim E_b^{-\gamma}$ for small E_b. The closer the G_M is to the critical value, the stronger the singularity. The dashed lines show the prediction of the SDE model $\gamma=1-a/D$. The fit is very good for small E_b; however, the SDE for a supercritical bifurcation fails to reproduce the peak of the PDF at large E_b due to the long duration of the on phases.

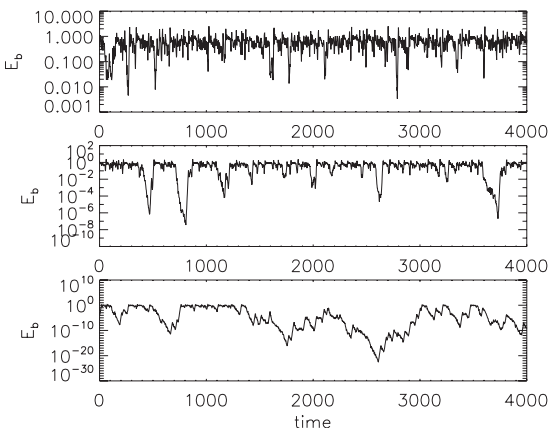

FIG. 8. Evolution of the magnetic energy for Gr=25 and G_M=41.6 (top panel), 35.7 (middle panel), and 31.2 (bottom panel).

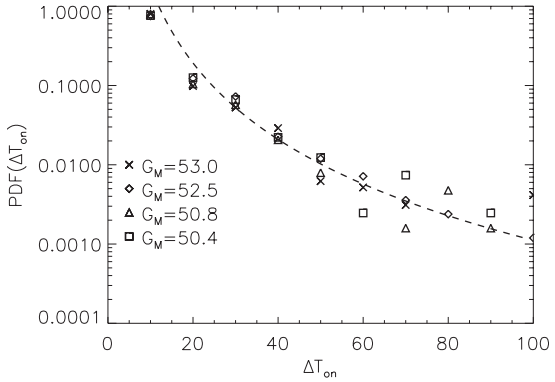

FIG. 9. Distribution of the on times for the Gr=39.06 case and three different values of G_M. The fit (dashed line) corresponds to the power law behavior $\Delta T^{-3.2}$. Here, the on time is considered to be the time that the dynamo has magnetic energy $E_b > 0.2$.

Another prediction of the SDE model is that all the moments of the magnetic energy $\langle E_b^m \rangle = \int f_{\text{PDF}}(E_b) E_b^m dE_b$ have a linear scaling with the deviation of G_M from the critical value G_{Mc} provided that the difference $G_M - G_{Mc}$ is sufficiently small. This result is based on the assumption that the singular behavior close to $E_b=0$ gives the dominant contribution to the PDF, which is always true provided that the ratio a/D is sufficiently small. However, if the system spends long times in the on phase, the range of validity of the linear scaling of $\langle E_b \rangle$ with $a \sim G_M - G_{Mc}$ is restricted to very small values of the difference $G_M - G_{Mc}$. Figure 11 shows the time-averaged magnetic energy $\langle E_b \rangle$ as a function of the relative difference $(G_M - G_{Mc})/G_M$ in a log-log scale. The dependence of $\langle E_b \rangle$ on the deviation of G_M from the critical value appears to approach the linear scaling, albeit very slowly. The best fit from the six smallest values of G_M shown in Fig. 11 gave an exponent of 0.8 [e.g.,

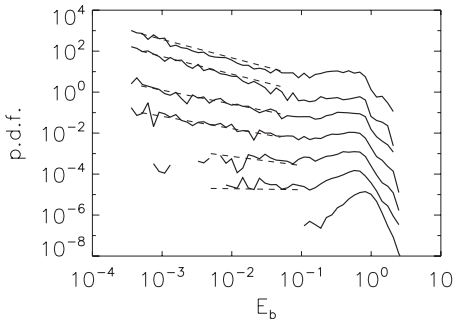

FIG. 10. Probability distribution functions of E_b, for Gr=25 and seven different values of G_M (starting from the top line, G_M=31.2, 33.3, 35.7,38.4, 41.6, 50.0, and 83.3. The last case G_M=83.3 shows no on-off intermittency. The dashed lines show the prediction of the SDE model. The PDFs have not been normalized for reasons of clarity.

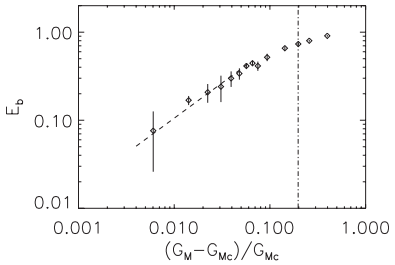

FIG. 11. Averaged magnetic energy as a function of the relative deviation from the critical magnetic Reynolds number. The dash-dotted vertical line indicates the location of $(G_{Mo}-G_{Mc})/G_{Mc}$, beyond which on-off intermittency is no longer present.

$\langle E_b\rangle \sim (G_M-G_{Mc})^{0.8}$]. The small difference from the linear scaling [$\langle E_b\rangle \sim (G_M-G_{Mc})^1$] is probably because not sufficiently small deviations (G_M-G_{Mc}) were examined. We note, however, that there is a strong deviation from the linear scaling for values of G_M close to G_{Mo}.

Of particular interest to the experiments is how the range of intermittency changes as Gr is increased. Typical Gr numbers for the experiments are of the order of $\mathrm{Gr}\sim \mathrm{Re}^2 \sim 10^{12}$ which it is not currently possible to obtain in numerical simulations. In Fig. 2 we showed the critical magnetic Reynolds number G_{Mc} for which dynamo instability is observed and the critical magnetic Reynolds number G_{Mo} where the on-off intermittency is present. G_{Mc} was estimated by interpolation between the run with the smallest positive growth rate and and the run with the smallest (in absolute value) negative growth rate. The on-off intermittency range was based on the PDFs of the magnetic energy. Runs for which the PDF had singular behavior at $E_b \simeq 0$ are considered on-off while runs with smooth behavior at $E_b \simeq 0$ are not considered to show on-off intermittency. The slopes of the PDF s (in log-log scale) for small E_b were calculated and the transition point G_{Mo} was determined by interpolation of the two slopes (see, for example, the bottom two curves in Fig. 10). In Fig. 12 we show the ratio $(G_{Mo}-G_{Mc})/G_{Mc}$ as a function of G_r, which expresses the relative range where on-off intermittency is observed. The error bars correspond to the smallest examined values of G_M where no on-off intermittency was observed (upper error bar) and the largest examined values of G_M where on-off intermittency was observed (lower error bar). The range of on-off intermittency is decreasing as Gr is increased, probably reaching an asymptotic value. However, to clearly determine the asymptotic behavior of G_{Mo} with Gr would require higher resolution, which the long duration of these runs does not allow us to obtain.

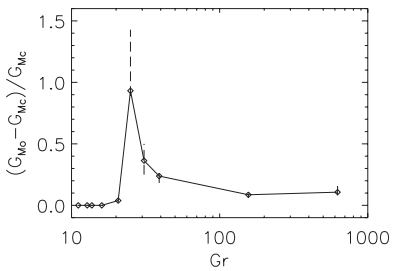

FIG. 12. The ratio $(G_{Mo}-G_{Mc})/G_{Mc}$ as a function of G_r that expresses the relative range for which on-off intermittency is observed. The upper limits of the error bars (dashed line) correspond to the smallest examined values of G_M for which no on-off intermittency was observed, and the lower limits of the error bars correspond to the largest examined values of G_M for which on-off intermittency was observed.

IV. DISCUSSION

In this work we have examined how the on-off intermittency behavior of a dynamo near criticality is changed as the kinematic Reynolds number is varied, and the effect of the Lorentz force in the nonlinear stage of the dynamo. The predictions of [30–33], linear scaling of the averaged magnetic energy with the deviation of the control parameter from its critical value, fractal dimensions of the bursts, distribution of the off time intervals, and singular behavior of the PDF of the magnetic energy, which were tested numerically in [21,22], were verified for a larger range of kinematic Reynolds numbers when on-off intermittency was present. Note, however, that all these predictions are based on the statistics of the flow in the kinematic stage of the dynamo. However, it was found that the Lorentz force can drastically alter the on-off behavior of the dynamo in the nonlinear stage by quenching the noise. For small Reynolds numbers, the Lorentz force can trap the original chaotic system in the linear regime into a time-periodic state, resulting in no on-off intermittency. At larger Reynolds numbers $\mathrm{Gr}>20$, on-off intermittency was observed but with long durations of the on phases that have a power law distribution. These long on phases result in a PDF that peaks at finite values of E_b. This peak can be attributed to the presence of a subcritical instability or to the quenching of the hydrodynamic noise at the nonlinear stage, or possibly a combination of the two. In principle, the SDE model [Eq. (1)] can be modified to include these two effects: a nonlinear term that allows for a subcritical bifurcation and an E_b-dependent amplitude of the noise. There are many possibilities to model the quenching of the noise; however, the nonlinear behavior might not have a universal behavior and we do not attempt to suggest a specific model.

The relative range of the on-off intermittency was found to decrease as the Reynolds number was increased, possibly reaching an asymptotic regime. However, the limited number of Reynolds numbers examined did not allow us to give a definite prediction for this asymptotic regime. This question is of particular interest for dynamo experiments [2–8], which until very recently [26] have not detected on-off intermittency. There are many reasons that could explain the absence of detectable on-off intermittency in the experimental setups, like the strong constraints imposed on the flow [4,5], which do not allow the development of large-scale fluctuations, or the Earth's magnetic field, which imposes a lower threshold for the amplitude of the magnetic energy. Numerical investigations at higher resolution and a larger variety of flows or forcing would be useful at this point to obtain a better understanding.

ACKNOWLEDGMENTS

We thank F. Pétrélis and J-F Pinton for fruitful discussions. A.A. acknowledges financial support from the Observatoire de la Côte d'Azur and the Rotary Clubs district 1730. Y.P. thanks the CNRS Dynamo GdR, INSU/PNST, and INSU/PCMI Programs. Computer time was provided by IDRIS, and the Mesocenter SIGAMM machine, hosted by Observatoire de la Cote d'Azur.

[1] H. K. Moffatt, *Magnetic Field Generation in Electrically Conducting Fluids* (Cambridge University Press, Cambridge, U.K., 1978); F. Krause and K.-H. Radler, *Mean-Field Magnetohydrodynamics and Dynamo Theory* (Pergamon, Oxford, 1980); E. N. Parker, *Cosmical Magnetic Fields* (Clarendon, Oxford, 1979).
[2] A. Gailitis *et al.*, Phys. Rev. Lett. **84**, 4365 (2000).
[3] A. Gailitis, O. Lielausis, E. Platacis, S. Dementev, A. Cifersons, G. Gerbeth, T. Gundrum, F. Stefani, M. Christen, and G. Will, Phys. Rev. Lett. **86**, 3024 (2001).
[4] A. Gailitis *et al.*, Phys. Plasmas **11**, 2838 (2004).
[5] U. Müller and R. Stieglitz, Naturwiss. **87**, 381 (2000).
[6] R. Stieglitz and U. Müller, Phys. Fluids **13**, 561 (2001).
[7] R. Monchaux *et al.*, Phys. Rev. Lett. **98**, 044502 (2007).
[8] M. Berhanu *et al.*, Europhys. Lett. **77**, 59001 (2007).
[9] P. Odier, J.-F. Pinton, and S. Fauve, Phys. Rev. E **58**, 7397 (1998).
[10] N. L. Peffley, A. B. Cawthorne, and D. P. Lathrop, Phys. Rev. E **61**, 5287 (2000).
[11] N. L. Peffley *et al.*, Geophys. J. Int. **142**, 52 (2000).
[12] P. Frick *et al.*, Magnetohydrodynamics **38**(1/2), 143 (2002).
[13] M. Bourgoin *et al.*, Phys. Fluids **14**, 3046 (2002).
[14] M. D. Nornberg, E. J. Spence, R. D. Kendrick, C. M. Jacobson, and C. B. Forest, Phys. Rev. Lett. **97**, 044503 (2006).
[15] M. D. Nornberg *et al.*, Phys. Plasmas **13**, 055901 (2006).
[16] R. Stepanov, R. Volk, S. Denisov, P. Frick, V. Noskov, and J.-F. Pinton, Phys. Rev. E **73**, 046310 (2006).
[17] R. Volk, P. Odier, and J-F Pinton, Phys. Fluids **18** 085105 (2006).
[18] M. Bourgoin *et al.*, New J. Phys. **8**, 329 (2006).
[19] Y. Pomeau and P. Manneville, Commun. Math. Phys. **74**, 189 (1980).
[20] N. Platt, E. A. Spiegel, and C. Tresser, Phys. Rev. Lett. **70**, 279 (1993).
[21] D. Sweet, E. Ott, J. M. Finn, T. M. Antonsen, Jr., and D. P. Lathrop, Phys. Rev. E **63**, 066211 (2001).
[22] D. Sweet, E. Ott, T. M. Antonsen, Jr., D. P. Lathrop, and J. M. Finn, Phys. Plasmas **8**, 1944 (2001).
[23] A. S. Pikovsky, Z. Phys. B: Condens. Matter **55**, 149 (1984); P. W. Hammer, N. Platt, S. M. Hammel, J. F. Heagy, and B. D. Lee, Phys. Rev. Lett. **73**, 1095 (1994); T. John, R. Stannarius, and U. Behn, *ibid.* **83**, 749 (1999); D. L. Feng, C. X. Yu, J. L. Xie, and W. X. Ding, Phys. Rev. E **58**, 3678 (1998); F. Rodelsperger, A. Cenys, and H. Benner, Phys. Rev. Lett. **75**, 2594 (1995).
[24] N. Leprovost, B. Dubrulle, F. Plunian, Magnetohydrodynamics **42**, 131 (2006).
[25] Y. Ponty, J.-P. Laval, B. Dubrulle, F. Daviaud, and J.-F. Pinton, Phys. Rev. Lett. **99**, 224501 (2007).
[26] J. Pinton, private communication.
[27] H. Fujisaka and T. Yamada, Prog. Theor. Phys. **74**, 918 (1985); H. Fujisaka, H. Ishii, M. Inoue, and T. Yamada, *ibid.* **76**, 1198 (1986).
[28] E. Ott and J. C. Sommerer, Phys. Lett. A **188**, 39 (1994).
[29] L. Yu, E. Ott, and Q. Chen, Phys. Rev. Lett. **65**, 2935 (1990).
[30] N. Platt, S. M. Hammel, and J. F. Heagy, Phys. Rev. Lett. **72**, 3498 (1994).
[31] J. F. Heagy, N. Platt, and S. M. Hammel, Phys. Rev. E **49**, 1140 (1994).
[32] S. C. Venkataramani, T. M. Antonsen, Jr., E. Ott, and J. C. Sommerer, Phys. Lett. A **207**, 173 (1995).
[33] S. C. Venkataramani, T. M. Antonsen, Jr., E. Ott, and J. C. Sommerer, Physica D **96**, 66 (1996).
[34] S. Aumaître, F. Pétrélis, and K. Mallick, Phys. Rev. Lett. **95**, 064101 (2005).
[35] S. Aumaître, K. Mallick, and F. Pétrélis, J. Stat. Phys. **123**, 909 (2006).
[36] F. Cattaneo, D. W. Hughes, and E. J. Kim, Phys. Rev. Lett. **76**, 2057 (1996).
[37] E. Zienicke, H. Politano, and A. Pouquet, Phys. Rev. Lett. **81**, 4640 (1998).
[38] N. H. Brummell, F. Cattaneo, and S. M. Tobias, Fluid Dyn. Res. **28**, 237 (2001).
[39] V. I. Arnold, C. R. Hebd. Seances Acad. Sci. **261**, 17 (1965).
[40] T. Dombre, U. Frisch, J. M. Greene, M. Henon, A. Mehr, and A. Soward, J. Fluid Mech. **167**, 353 (1986).
[41] D. J. Galloway and M. R. E. Proctor, Nature (London) **356**, 691 (1992).
[42] Y. Ponty, A. Pouquet, and P. L. Sulem, Geophys. Astrophys. Fluid Dyn. **79**, 239 (1995).
[43] V. I. Arnold and E. I. Korkina, Vestn. Mosk. Univ. Mat. Mekh. **3**, 43 (1983).
[44] D. J. Galloway and U. Frisch, Geophys. Astrophys. Fluid Dyn. **36**, 53 (1986).
[45] B. Galanti, P. L. Sulem, and A. Pouquet, Geophys. Astrophys. Fluid Dyn. **66**, 183 (1992).
[46] V. Archontis, S. B. F. Dorch, and A. Nordlund, Astron. Astrophys. **397**, 393 (2003).
[47] R. Teyssier, S. Fromang, and E. Dormy, J. Comput. Phys. **218**, 44 (2006).
[48] S. Childress and A. D. Gilbert, *Stretch, Twist, Fold: The Fast Dynamo* (Springer, New York, 1995).
[49] H. K. Moffatt and M. R. Proctor, J. Fluid Mech. **154**, 493 (1985).
[50] B. J. Bayly and S. Childress, Geophys. Astrophys. Fluid Dyn. **44**, 211 (1988).
[51] J. M. Finn and E. Ott, Phys. Fluids **31**, 2992 (1988).
[52] J. M. Finn and E. Ott, Phys. Rev. Lett. **60**, 760 (1988).
[53] O. M. Podvigina and A. Pouquet, Physica D **75**, 471 (1994).
[54] O. M. Podvigina, Physica D **128**, 250 (1999).
[55] P. Ashwin and O. Podvigina, Proc. R. Soc. London, Ser. A **459**, 1801 (2003).
[56] O. Podvigina, P. Ashwin, and D. J. Hawker, Physica D **215**, 62 (2006).
[57] P. D. Mininni, Phys. Plasmas **13**, 056502 (2006).